Phase separation studies in RIM polyurethanes catalyst and hard segment crystallinity effects*

R. E. Camargo,† C. W. Macosko, M. Tirrell and S. T. Wellinghoff‡
Department of Chemical Engineering and Materials Science, University of Minnesota, Minneapolis, Minnesota 55455, USA
(Received 17 May 1984; revised 10 August 1984)

Polyurethanes were prepared from pure 4,4'-diphenylmethane diisocyanate (MDI), 1,4-butane diol (BDO) or 1,2-ethane diol (EDO) and α,ω-hydroxyl poly(propylene oxide) (PPO) by reaction injection moulding (RIM). Hard segment (MDI + BDO or EDO) level was 45–50 wt%. The PPO had about 20% ethylene oxide copolymerized in at the chain ends to provide 80% primary OH end groups. M_n was varied from 2000 to 4000. Dibutyl tin dilaurate catalyst and mould temperature were varied. Dynamic mechanical, wide-angle X-ray, differential scanning calorimeter, molecular weight and tensile elongation measurements were made on the RIM polyurethanes. At low reaction rates (low catalyst or temperature) highly crystalline, well phase separated but low molecular weight polymers were produced. At high catalyst or temperature levels more poorly phase separated but high molecular weight, tough polymers resulted. Higher M_n PPO gave better phase separation and EDO gave higher melting temperatures. Preventing hard segment crystallinity by substituting asymmetric MDI or glycols resulted in phase compatibility.

(Keywords: polyurethane; reaction injection moulding; polymerization rate; molecular weight; phase separation; crystalline hard segments)

INTRODUCTION

Production of polyurethane elastomers by reaction injection moulding, RIM, is now a well established technique. Since RIM involves a fast exothermic polymerization, the development of structure and properties in the materials thus produced is constrained by processing and polymerization conditions. The particular properties of polyurethane elastomers derive to a large extent from phase separation into hard, crystalline or glassy regions that reinforce the soft rubbery phase. *Figure 1* gives a simplified representation of such a microstructure. The hard segments are composed of sequences of a diisocyanate reacted with a short chain diol or diamine, the extender. In the particular instance of *Figure 1*, the hard segments are shown as crystalline, but they can also be amorphous. The soft segments are composed primarily of a long chain diol or triol (equivalent weight of 1000 or greater), and also of diisocyanate-extender sequences scattered throughout the matrix.

Major factors affecting the final properties of the polymer are the composition and the degree of order within each phase, and the topology or connectivity of the microphase structure, i.e. sharpness of the domain boundaries and mixing of the phases.

Several studies have been published in recent years on the properties of RIM polyurethanes and polyurethane–ureas[1–7]. Unlike most studies, however, we have restricted our attention to simplified linear systems in order to establish the effect of reaction rates and mould temperatures on the phase separation and molecular weight of segmented polyurethane elastomers produced by RIM[6].

In our earlier work, we prepared rapidly polymerized samples with high molecular weight and finely dispersed hard and soft phases of low hard segment crystallinity. A high temperature sensitivity of the storage modulus was characteristic of this structure. At low reaction rates the polymerization proceeded almost isothermally at large undercooling. Incompletely reacted, low molecular weight, oligomers of high hard segment content phase separated into large spherulitic structures, between which was isolated material of rather low fracture strength. Evidently, early formation of hard segment crystallites can remove unreacted isocyanate groups from solution preventing further reaction with the polyol[6,8].

SCOPE OF THE PRESENT WORK

We have extended our previous experiments[6] to a wider spectrum of catalyst concentrations, at hard segment levels typical of those used in the production of RIM fascia automobile parts* (e.g. 45–50% hard segment). As in our previous work, only difunctional reactants at matched stochiometries of the reactants have been used. This ensures linear, soluble polymers and allows molecular weight characterization.

* Presented in part at the American Chemical Soc. meeting, Washington, D.C., August 1983. Reprinted with permission from Camargo, R. E. *et al.* in 'Reaction Injection Molding: Polymer Chemistry and Engineering', (Ed. Jiri Kresta), ACS Symposium Series No. 270; American Chemical Society, Washington DC, p. 27. Copyright 1985 American Chemical Society.

†Present address: Raychem Corporation, Corporate Technology, Menlo Park, CA 94025.
‡Present address: South West Research, San Antonio, Texas 78238, USA

* In this paper, the hard segment content is defined as the per cent by weight of the isocyanate and extender in the polymer at a fixed stochiometry or isocyanate index.

0032-3861/85/081145-10$03.00

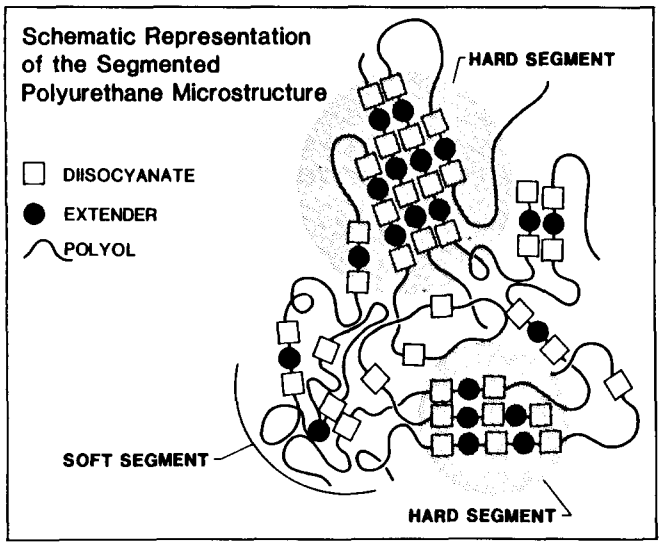

Figure 1 Schematic representation of the segmented microstructure in a semicrystalline polyurethane block copolymer

To study the role of hard segment crystallizability, two series of polymers were prepared from special reactants as described in the Experimental section. In addition some comparative results have been obtained by varying the molecular weight of the polyols used.

EXPERIMENTAL

Materials

The polyurethanes used are based on poly(propylene oxide diol), capped with a certain amount of poly(ethylene oxide) to provide high primary hydroxy content, and thus high reactivity. The main characteristics of the polyols are listed in *Table 1*. Crystallizable hard segments were made from 4,4′-diphenylmethane diisocyanate, MDI (Rubinate 44, Rubicon Chemicals) and 1,4-butanediol, BDO (GAF Chemicals) or 1,2-ethanediol, EDO (ethylene glycol, Fisher Scientific). Amorphous hard segments were obtained using 2,4′-diphenylmethane diisocyanate, 24-MDI (this non-commercial material was kindly provided by Dr D. Spence from Rubicon Chemicals) and BDO, or 44-MDI and n-methyldiethanol amine, MDEA (Union Carbide Corp.). In either case hard segment crystallization is inhibited by molecular asymmetry (24-MDI/BDO) or by branching (MDI/MDEA). The catalyst used in all cases was dibutyltin dilaurate, DBTDL (T-12, M. & T. Chemicals).

Sample identification

Given the number of samples and compositions, a general code was created as explained in *Table 2*. In this Table, the polyol type is identified by molecular weight and ethylene oxide content. Thus 40/15 refers to a polyol with $M_n \approx 4000$ and 15% (w/w) of ethylene oxide end-capping agent. The last two labels in *Table 2* indicate mould temperature and catalyst content.

Reaction injection moulding

Moulded polymer samples were produced in our laboratory-size RIM machine[9]. Details of reactant preparation and moulding procedures are found elsewhere[9,10]. Briefly, the polyol and extender were blended as received at the desired stochiometry. Catalyst was added when required and the mixture subsequently degassed at room temperature for approximately eight hours. The pure MDI was melted and filtered at *ca.* 50°C immediately before each run. The chemicals were loaded in the machine tanks and blanketed with nitrogen. All lines and tanks were kept at 55°C ± 5°C at all times. During the injection cycle, the materials were injected at the rate of *ca.* 0.1 kg s^{-1} through a recirculating, self-cleansing, impingement mixing head, and into a rectangular, end-gated, teflon-coated mould (125 × 125 × 3 mm), opened and closed by a hydraulic press. Mould temperature was maintained by means of electrical resistances. The mould temperature in most runs was kept at 70°C. After demoulding, the polymer plaques were postcured in an oven at 120°C for 1 hour, and aged at room temperature for at least one week prior to analysis.

Dynamic mechanical spectroscopy (DMS)

Rectangular bars (3 × 12 × 45 mm) were cut from the moulded plaques and dynamic mechanical spectra (DMS) obtained using a Rheometrics System-4. Values of G', G'' and $\tan\delta$ at various temperatures were obtained by oscillatory torsion of the bars at 1 Hz and 0.2% shear strain; temperatures were varied between −100°C and 120°C at 5°C intervals in the transition regions and at 10°C intervals elsewhere. Thermal soak times were five minutes in all cases.

Wide-angle X-ray scattering

WAXS data were obtained on 25 × 25 × 3 mm samples; reflected intensity was recorded as a function of scattering angle (2θ) at 1° min^{-1}, with a Siemens D500 diffractometer, using monochromated Cu-K radiation.

Differential scanning calorimetry

D.s.c. scans were made at 20°C min^{-1} on a Mettler TA3000 system equipped with a DSC-30 low temperature module. Temperature calibration was done with a multiple indium–lead–nickel standard. An indium standard

Table 1 Characteristics of polyols used

Commercial name	Supplier	M_n[a,b]	M_w/M_n[c]	%(w) EO[b]	% Primary OH's[b]	Identification code[d]
Niax 1256 (special)	Union Carbide Corp.	1999	1.11	30.4	83	20/30
Niax E-351	Union Carbide Corp.	2772	1.15	~15	75–80	28/15
Thanol E2103	Texaco Chemicals	2306	1.12	25	80	23/25
Poly G 55-28	Olin Corporation	4080	1.20	~15	80–85	40/15

[a] Calculated assuming hydroxyl functionality of two
[b] Data from supplier
[c] From g.p.c. measurements
[d] Corresponds to (M_n/100)/(%EO)

Table 2 A sample identification code
(A) Chemical code and range of variables

Isocyanate type	Extender type	Polyol type	Hard segment (%)[a]	Mould temperature (°C)	Catalyst content 1000 × % cat
MDI = M	BDO = B	20/30	48	70	00
	EDO = E	23/25			
	MDEA = M	28/15	to	to	to
24-MDI = 24M		40/15			
			51	140	75

[a] Defined in text

(B) An example: M – E – 23/25 – 48 – 70 – 30

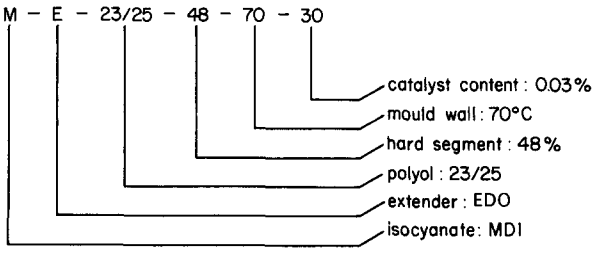

was used for heat flow calibration. Thin shavings (*ca.* 0.5 mm thick) were cut with a razor blade from the cross-sectional edge of a plaque. These sections contained both surface and centre portions.

Gel permeation chromatography

A Waters (model 150-C ALC/GPC) liquid chromatograph with a refractive index detector was used for molecular weight characterization. The unit was equipped with two sets of silanized Dupont bimodal columns (Zorbax PSM 60S/1000S), with molecular weight range 2×10^2 to 10^6 and total retention volume of 24 ml. Samples were cut across the plaque thickness as with d.s.c. Polymer solutions were prepared in *N,N'*dimethylformamide, DMF, at 0.1% (w/v) and filtered through 0.45 micron nylon filters (Rainin Instruments). Injection volume was 0.2 ml and the solvent temperature in the columns was 80°C. Flow rate was adjusted between 0.5 and 1.0 ml min^{-1} to keep the pressure at *ca.* 80% of the maximum pressure setting (16 MPa). The data for each run were continuously fed to a PDP 11/60 computer for storage and further analysis. Calculations were done using a polystyrene standard calibration, since polyurethane calibrations are currently unavailable.

Mechanical properties

Stress–strain curves for two of the series studied M-B-40/15-49 and M-E-23/25-48 were done at Rubicon Chemicals (Woodbury, NJ), using the ASTM D-412 method (tensile properties of rubbers) at a strain rate of 500 mm min^{-1}. Young's modulus was determined from the initial slope of the stress–strain curve of two to four samples.

RESULTS

Dynamic mechanical spectra

Dynamic shear moduli, *G'* and *G''* for BDO and EDO based materials are shown in *Figures 2* to *4*. For the 23/25 polyol, increased reaction rate (catalyst) leads to greater temperature sensitivity of the storage modulus in the rubbery region. As in our previous findings[6], overall

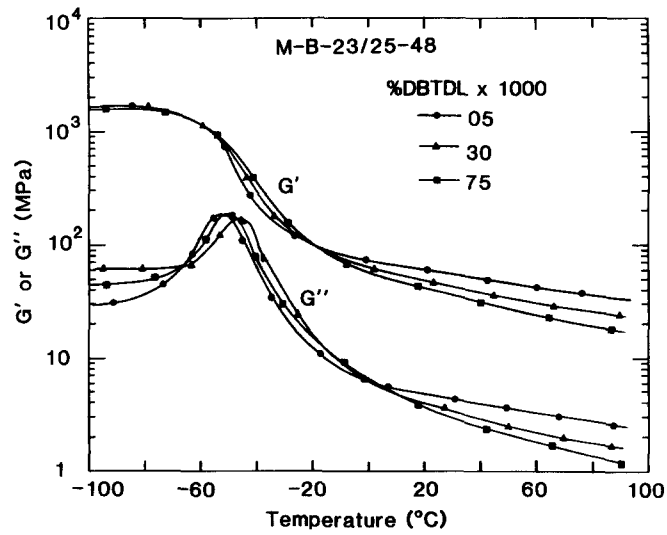

Figure 2 Dynamic mechanical properties for the M-B-23/25-48 series as a function of catalyst concentration

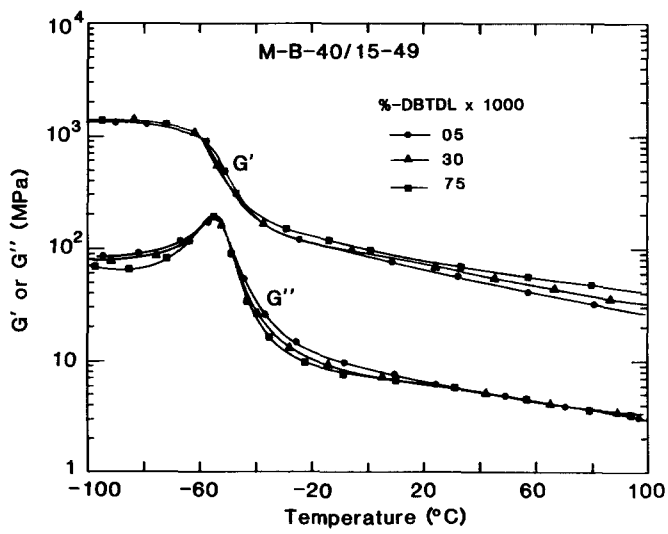

Figure 3 Dynamic mechanical properties for the M-B-40/15-49 series as a function of catalyst concentration

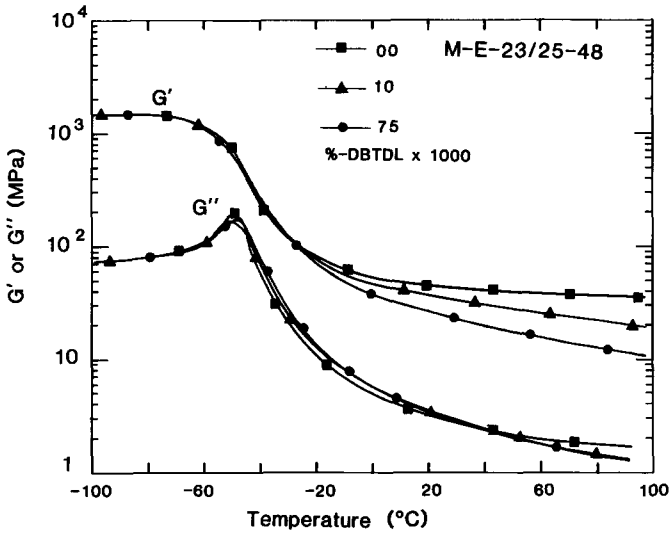

Figure 4 Dynamic mechanical properties for the M-E-23/25-48 series as a function of catalyst concentration

phase separation seems to be improved by lower reaction rates. Increasing polyol molecular weight to 4000 reduces differences in the modulus temperature behaviour as a function of catalyst composition (cf. *Figure 3*).

Unlike in our earlier work[6] very few differences were observed in the glass transition temperature of the soft segments T_{gs} as a function of catalyst content. Similar results were obtained by d.s.c. (as discussed later). An increase in the polyol molecular weight, on the other hand, decreased the T_{gs} significantly (*Figure 5*). The T_g values obtained by d.s.c., however, were about 10° lower than DMS data. Similar differences were found by Zdrahala *et al.*[11,12] and Russo and Thomas[13].

We studied two factors which affect dynamic moduli vs. temperature behaviour: catalyst concentration, or equivalently, reaction speed, and polyol molecular weight. One way of comparing the data is to look at the $G'(-30°C)/G'(70°C)$ ratio. This is a measurement of the flatness of the rubbery plateau. The two temperatures are rather arbitrary but they can be taken as practical limits of use for these elastomers, at least in automotive applications. *Figure 6* shows the effect of catalyst concentration on the ratio $G'(-30°C)/G'(70°C)$ of different series. Higher catalyst content products a polymer with more modulus temperature sensitivity. For the sake of completeness the series M-B-20/30-60 studied earlier[6] has been added. *Figure 7* shows that polyol molecular weight decreases $G'(-30°C)/G'(70°C)$. We interpret this as an increase in the degree of phase separation. We would expect this trend to level off at higher molecular weight polyols.

Amorphous systems

The linear viscoelastic properties of the amorphous series (M-M-23/25-51 and 24M-B-23/25-48) are very different from the ones discussed so far in that the T_{gs}'s are *ca.* 30°C higher than those found in semicrystalline MDI-BDO or MDI-EDO based systems.

In *Figure 8* we compare G' and G'' for samples produced under similar conditions from symmetric and asymmetric MDI isomers. The storage modulus of the 24-MDI based material drops by about three orders of magnitude after T_{gs}. Above 50°C, dynamic mechanical measurements were discontinued due to extreme softening of the samples. G' and G'' vs. T curves for the MDEA based materials are similar to those of the 24-MDI shown in *Figure 8*.

Wide-angle X-ray diffraction

Scattered intensity vs. angle WAXS curves for MDI-BDO based materials were similar to those previously reported by us[6] and other investigators[14,15] (cf. *Figure 9a*). Again, at low catalyst concentrations, prominent reflections are observed; as catalyst concentration increases, the intensity of the sharp reflections decreases until almost an amorphous looking pattern is observed in very fast systems (e.g. 0.075% DBTDL). The MDI–EDO materials display similar behaviour. With no catalyst, there are strong crystalline reflections at 3.41, 3.88, 4.23, 4.75, 7.82 and 15.5 Å (cf. *Figure 9b*). These *d*-spacings are in good agreement with those recently reported by Turner *et al.*[7] on similar systems. As catalyst concentration increases, most reflections are gradually weakened. However, some reflections still appear at very high catalyst concentrations (*Figure 9b*).

The MDEA and 24-MDI based samples display WAXS intensity curves characteristic of amorphous systems, thus confirming the absence of three dimensional order in the domains.

Differential scanning calorimetry

D.s.c. scans for the M-B-23/25-48 series are shown in *Figure 10*. At low catalyst concentrations, there are two prominent endotherms at *ca.* 215°C and 225°C. As catalyst content increases, a new broad endotherm appears at *ca.* 190°C. These endotherms are characteristic of all polyol systems polymerized at high catalyst concentrations and/or high mould temperatures (*Figure 11*). Multiple endotherms in MDI/BDO polymers have been previously reported by other investigators (e.g. refs. 4, 14, 16, 17). Overall heats of fusion are a measure of crystallinity and crystal perfection and size and were higher (24 J/g) for samples with low catalyst content.

Figure 12 shows the d.s.c. scans for the M-E-23/25-48 series are a function of DBTDL concentration. In general the multiple melting points for the MDI–EDO based hard

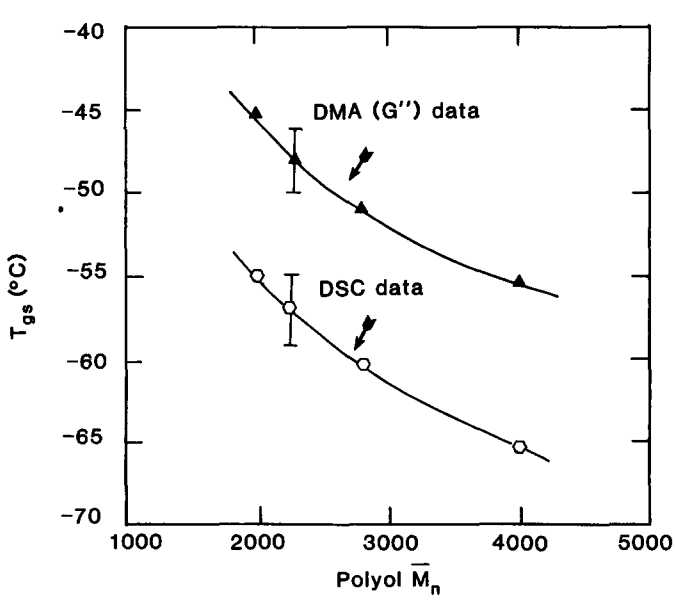

Figure 5 Soft segment glass transition temperature, T_{gs}, as a function of polyol molecular weight

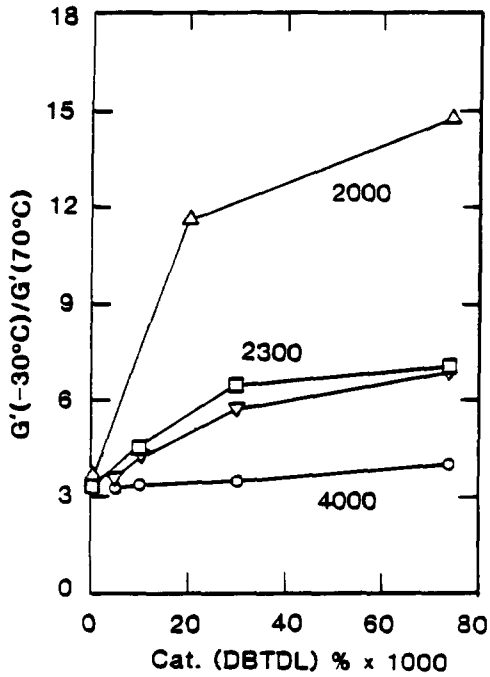

Figure 6 Modulus ratio, $G'(-30°C)/G'(70°C)$ *versus* concentration of DBTDL catalyst. (△) M-B-20/30-60, (▽) M-B-23/25-48; (○) M-B-40/15-49; (□) M-E-23/25-48

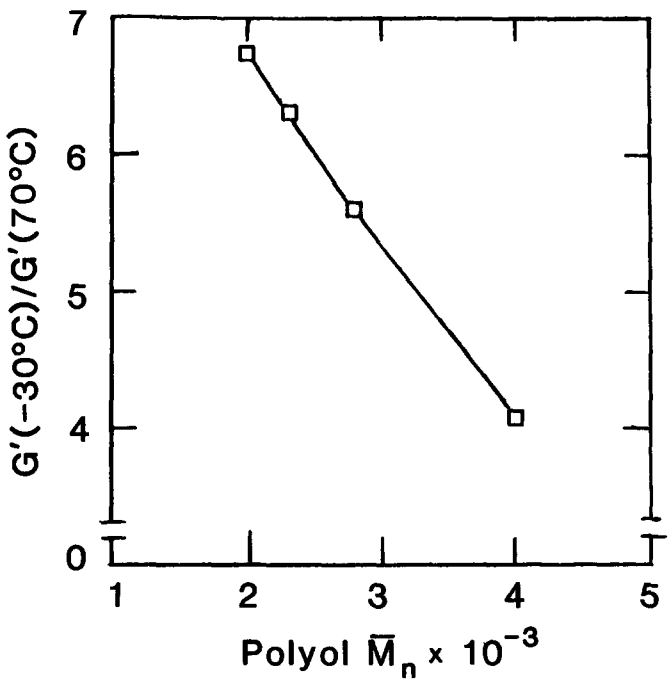

Figure 7 Effect of polyol M_n on the modulus ratio, $G'(-30°C)/G'(70°C)$, M-B series

segments are higher than the MDI–BDO based materials. Dominguez[4] also reports higher melting points in RIM materials produced from EDO and uretonimine modified MDI. However, his temperatures are below ours made with pure MDI. Heats of reaction in the MDI–EDO samples were somewhat higher than those of the MDI–BDO counterparts. The heat of fusion of the uncatalysed composition was significantly higher than that of the catalysed samples (40 J/g *versus* 25 J/g).

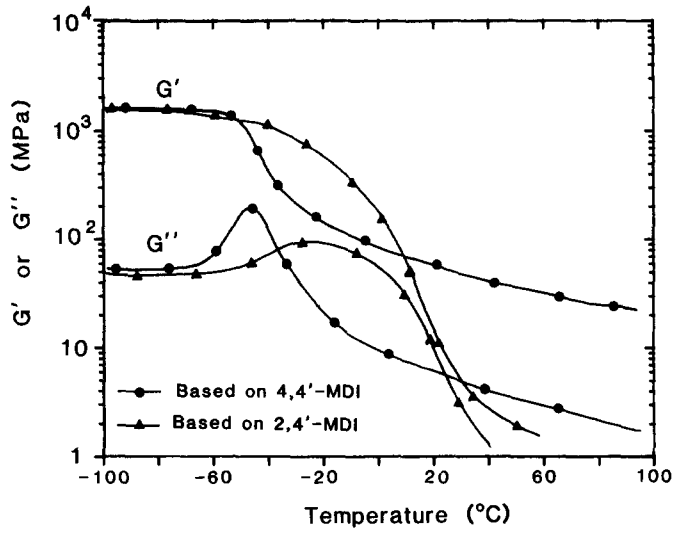

Figure 8 Comparison of dynamic mechanical properties for polyurethanes made from symmetric and asymmetric MDI isomers

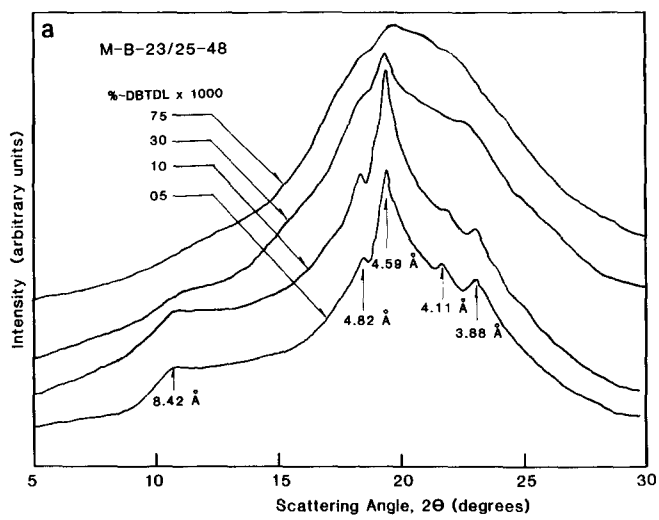

Figure 9a WAXS diffraction curves for the M-B-23/25-48 series at different levels of catalyst (DBTDL)

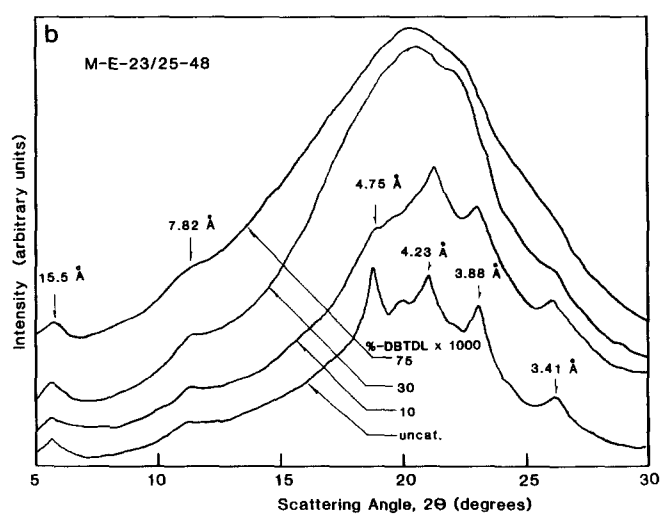

Figure 9b WAXS diffraction curves for the M-E-23/25-48 series at different levels of catalyst (DBTDL)

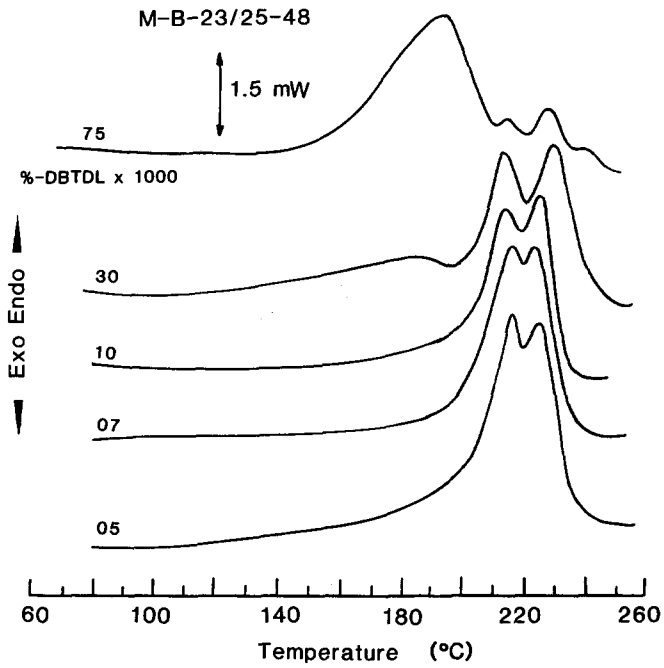

Figure 10 D.s.c. curves for the M-B-23/25-48 series at different concentrations of DBTDL catalyst

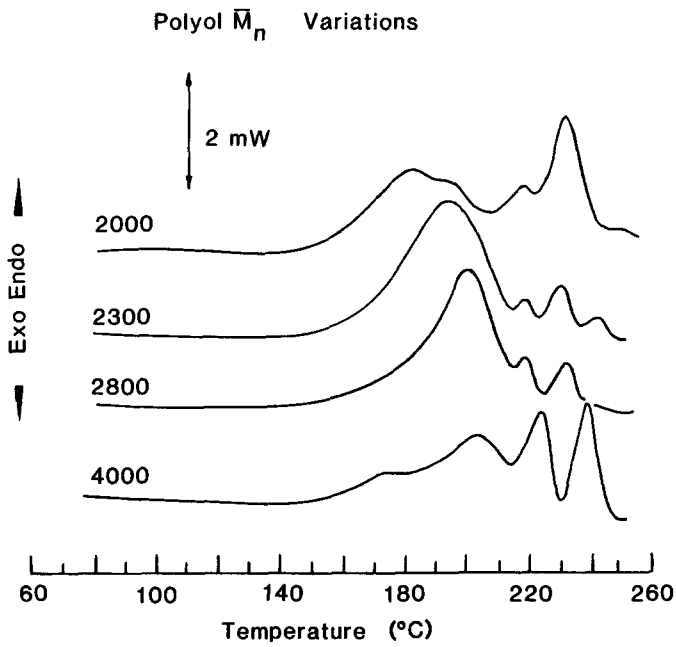

Figure 11 D.s.c. curves for different polyurethanes at 0.075% DBTDL (fast systems). Effect of the polyol M_n in M-B series

Molecular weight determination

As mentioned earlier, the g.p.c. results for our samples are based on a polystyrene calibration curve. As such, all numbers must be regarded on a relative basis. PS based weight average molecular weights, M_w, were about 10^5 for highly reacted samples. Actual M_w values may be lower even by a factor of 2, based on calculations for a stepwise polycondensation with 99% conversion[18]. M_w *versus* DBTDL concentrations for a typical series are shown in *Figure 13*. As observed the effect of a hotter mould wall at constant catalyst compositions is to increase the molecular weight of the sample. *Figure 14* compares the different series, with M_w's normalized by the highest value in the series. Except for the M-B-20/30-60 series in which the mould temperature was 100°C all other samples were moulded at 70°C.

All samples show a sharp decrease in M_w at 0.02–0.03% DBTDL. Judging from the results of the M-B-20/30-60 series, an increase in mould temperature allows for larger decreases in catalyst composition without major effect on the molecular weight. Information like this is valuable in establishing optimum levels of catalyst or moulding conditions.

The M_w of the amorphous samples were generally high (i.e. around 10^5). It is important to note that these results hold even for the uncatalysed sample of the M-M-23/25-51 series. In terms of reaction speed this sample is comparable to EDO or BDO based materials with *ca.*

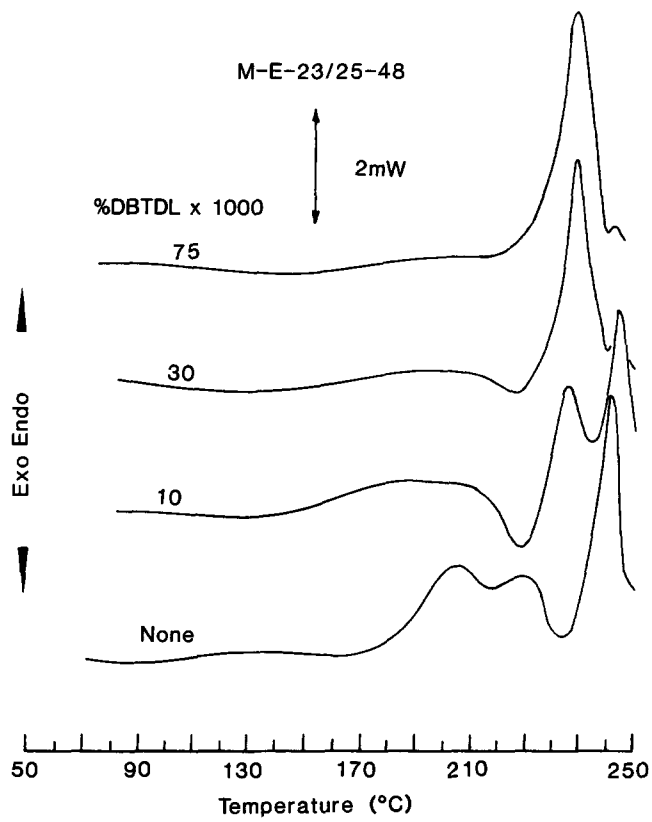

Figure 12 D.s.c. curves for the M-E-23/25-48 series at different concentrations of DBTDL catalyst

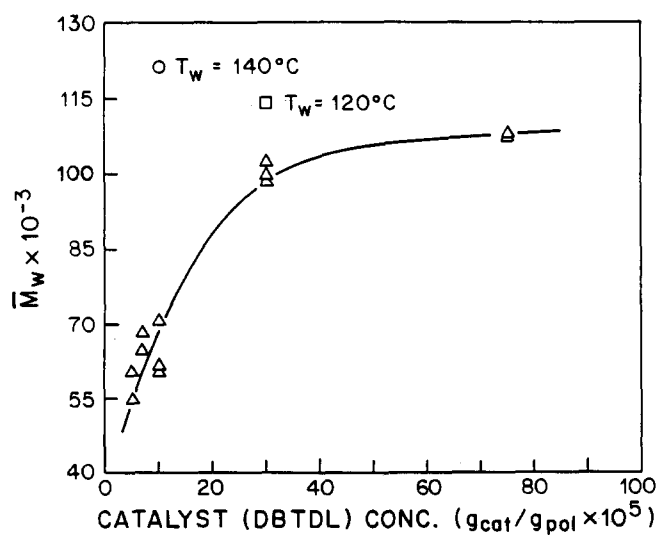

Figure 13 Molecular weight, M_w *versus* catalyst content for the M-B-23/25-48 series. Unless otherwise noted, mould temperature was 70°C

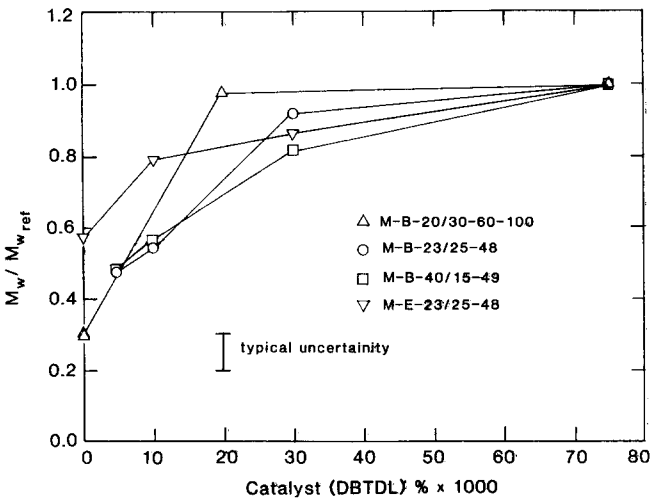

Figure 14 Normalized molecular weights, vs. catalyst concentration for different series. M_w ref. = value at highest catalyst

0.01–0.02% DBTDL, probably due to the presence of the catalytically active tertiary amine group in the MDEA molecule[10]. Nonetheless, the molecular weight is comparable to that of much faster samples. This, as we will discuss later is due to general absence of phase segregation during the reaction in the MDEA based materials.

A final and important observation must be made concerning molecular weight results. Ideally the polydispersity (M_w/M_n) of these samples should be close to 2.0. Indeed this was found in most samples with two remarkable exceptions. A decrease of catalyst content in the M-B-40/15-49 and M-E-23/25-48 series lead to higher polydispersity values. The uncatalysed sample of the M-E-23/25-48 series for instance had a polydispersity of 8.0. Moreover, the g.p.c. traces in these materials indicated the presence of shoulders. Upon close examination, at least one of the shoulders could be assigned to the polyol originally used in the composition, as seen in *Figure 15* for the M-E-23/25-48-70-00 sample. Similar results were observed for the M-B-40/15-49-70-05 sample.

Examples of high polydispersity ratios and bimodal distributions have been previously rationalized by heterogeneous reaction conditions. Tirrell *et al.*[19] found M_w/M_n values well over 2.0 and low molecular weight shoulders in slow, low temperature RIM polymerized urethanes based on polycaprolactone diols. Xu *et al.*[20] have recently performed selective extraction experiments on urethanes based on toluene diisocyanate, TDI, and hydroxyl terminated polybutadiene. They have shown that two different chain length distributions are a consequence of insoluble initial components.

Tensile properties

Stress–strain data for the M-E-23/25-48 series is shown in *Figure 16*. Elongations at break drop rapidly with lower DBTDL concentrations. Young's modulus was measured at about 42 MPa (6000 psi). Similar results were obtained in samples of the M-B-40/15-49 series where Young's modulus in this case was *ca.* 60 MPa (8700 psi).

It is important to compare these results to molecular weight data presented in the previous section. A drop in molecular weight of *ca.* 20% represents changes in elongation from 500% to 100%. Only those samples with 0.075% DBTDL display stress–strain data typical of elastomeric materials. Evidently in linear polyurethanes produced by RIM, only with high catalyst levels are molecular weights in the region where mechanical properties became insensitive to molecular weight[21]. This characteristic certainly justifies the use of triols or multifunctional isocyanates in commercial RIM systems, provided that morphology and domain formation are not significantly affected.

DISCUSSION

Crystalline systems

Lower T_{gs}, flatter rubbery plateau modulus, higher hard segment crystallinity, all support the view that phase separation is more complete in MDI–BDO and MDI–EDO based polyurethanes as catalyst concentration decreases.

Highly catalysed materials display a temperature sensitive plateau modulus and lower hard segment organization as evidenced by WAXS and d.s.c. data. These samples are flexible and tough with good tensile properties. Recent *RT* infra-red data indicates that there is a high degree of hard segment association through hydrogen bonding[10,22]. The evidence suggests that rapidly polymerized specimens can be viewed as a disperse, highly interconnected network of loosely organized hard segments reinforcing a polyether rich soft segment matrix. Additional arguments to support this hypothesis follow.

Hashimoto and coworkers[23] analysed the effects of interdomain mixing and phase boundary mixing (i.e. broader interphases) on the linear viscoelastic properties of block copolymers. Briefly, both mixing and interphase broadening increase the temperature dependence of the storage modulus. Changes on the loss modulus, however, are different in the two cases. Interdomain mixing results in shifts of the transition peaks toward each other with little or no broadening. Interphase boundary mixing, on the other hand, produces a broadening of the transition peaks but negligible shifts of the transition temperatures.

Based on the above interpretation, the main effect of increased catalyst concentration is to produce more diffuse boundaries between the hard and soft domains, since differences in T_{gs} among the samples are small, while

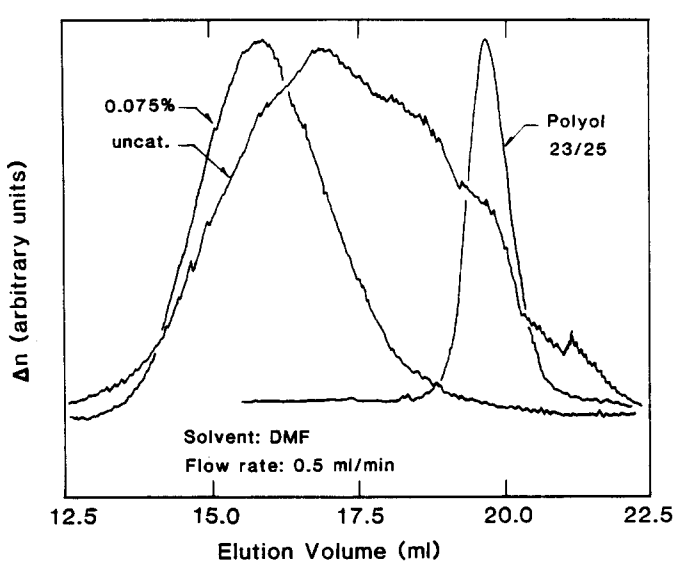

Figure 15 G.p.c. traces for catalysed (M-E-23/25-48-70-75) and uncatalysed (M-E-23/25-48-70-00) RIM samples and the starting polyol, 23/25. Note the correspondence between the shoulder in the uncatalysed sample and the polyol

differences in temperature dependency of the modulus are large as indicated by *Figure 6*. It is interesting to observe in this figure also that all curves converge to a limiting modulus ratio value of about 3.0, $G'(-30°C)/G'(70°C)$. A survey of literature data[5,12,24] indicates that for polyether urethane elastomers of similar hard segment concentration, the modulus ratio values are greater or equal to this limiting value. It is therefore reasonable to assume that 3.0 corresponds to a system that is completely phase separated with very sharp boundaries. In very slow systems this situation is accomplished by an early precipitation of mobile hard segment oligomers which form reasonable stable crystalline structures. However, there is a low degree of connectivity between hard and soft segments because the tight packing of the crystalline structures prevents further reaction of groups attached to crystalline chains.

As the reaction speed increases, high conversions can be achieved in a time interval shorter than the characteristic time for phase separation. Moreover, non-isothermal effects become important. Due to the exothermic nature of the reaction, the temperature of the reactive medium is greatly increased, possibly to the region of phase compatibilization. At this point the system can cool down, but domain formation is difficult due to high molecular weight and high viscosity. Thus only a finely interconnected structure results. Reduced segment mobility prevents the hard segments from reaching a high degree of crystalline organization.

Increasing the molecular weight of the polyol decreases the critical value of the interaction parameter χ_{AB} for phase separation and thus increases the driving force for phase separation. Hence the flatter modulus plateau in the samples of the M-B-40/15-48 series. Another variable that may also contribute to the higher degree of phase separation in the M-B-40/15-48 series is the lower ethylene oxide content of the polyol (*Table 1*). Since the poly(ethylene oxide) segment is more polar than the poly(propylene oxide) segments, we expect ethylene oxide to promote phase mixing. Recently, Kojima and coworkers[24] have shown that the temperature dependence of modulus in RIM urethanes increases as the content of ethylene oxide in a triol of constant equivalent weight increases.

The picture presented thus far is also supported by other experimental data. WAXS and d.s.c. data show that rapidly polymerized samples do not display a high degree of crystallinity in the hard segments. Annealing studies of some of our samples indicate that the broad peak at *ca.* 190°C can be slowly converted to a peak at *ca.* 220°C. If annealing is done at high enough temperature (210°C or higher), a new d.s.c. endotherm appears at *ca.* 235°C[10]. This is in agreement with recent work of Thomas and Briber[25] and Blackwell and Lee[26] who have independently proposed the existence of at least two different crystal structures in MDI–BDO based hard segments.

Perhaps one of the most important effects of a low reaction rate and premature phase separation is the decrease in molecular weight of the material. This clearly must be avoided as it seriously decreases the tensile properties of the polymer. There exists therefore a balance between the degree of phase separation and organization that can be achieved and the maximum molecular weight. As the latter has more importance regarding the performance of the material, it is necessary in real systems to turn to other alternatives such as the use of triols or graft polyols to increase molecular weight without seriously affecting the ability of the system to reach a certain degree of phase separation.

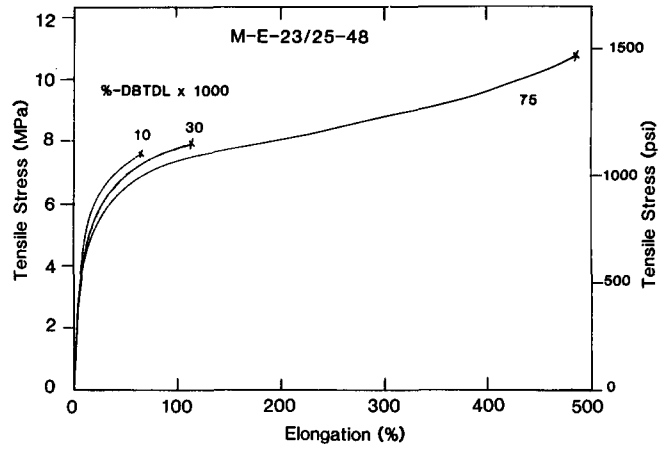

Figure 16 Stress–strain curves for the M-E-23/25-48 series as a function of catalyst concentration

Finally, a word must be said regarding spacial variations. In real samples, large temperature gradients develop during the polymerization. Generally monomers near the mould wall, react slower, and thus can undergo phase separation at an early stage, decreasing the local molecular weight of the material. Centre to surface variation tend to be magnified at intermediate catalyst concentrations (e.g. 0.01 to 0.05% DBTDL). At concentrations lower than these, the overall system is slow and early phase separation occurs throughout the part. At very high catalyst concentrations, the reaction is fast even near the mould wall. High conversions can be reached before appreciable phase separation can affect molecular weight. For this reason, surface to centre differences are also minimized (cf. ref. 6, *Figure 5*).

Non-crystalline systems

As inferred from the experimental data, those systems based on 24-MDI or MDEA are highly compatible and have a low modulus at room temperature. They display only a single T_g much higher than the one of the crystalline systems described in the previous section.

It is useful to compare the T_g values obtained for the amorphous M-M-23/25-51 and 24-M-B-23/25-48 series to predictions for random homogeneous systems. Using for instance Fox's equation[27]:

$$\frac{1}{T_g}=\frac{w_s}{T_{gs}}+\frac{w_h}{T_{gh}}$$

where w_s and w_h are the weight fractions of the soft (s) and hard (h) phases and T_{gs} and T_{gh} are the corresponding glass transition temperatures. T_{gs} for the polyethers used in this work is $-65°C$.[10] Hwang *et al.*[28] reported $T_{gh}=54°C$ for the MDI/MDEA hard segment. T_{gh} for the 24-MDI/BDO hard segments has been measured at 74°C using a copolymer polymerized in solution[10]. As observed from *Table 3*, the predictions of Fox's equation are in good agreement with the values measured in this work, indicating once again that these systems are highly compatible.

Summarizing then, the amorphous glycol extended systems have a large degree of phase compatibility and

Table 3 D.m.f. and d.s.c. data for glycol extended amorphous samples

Sample	T_g[a]	T_g[b]	T_g[c]	G' (−30°) (MPa)	$\frac{G'(-30°C)}{G'(70°C)}$
M-M-23/25-51-70-19	−12	−18.6	−18.7	794	>100
24M-B-23/25-48-70-150	−22	−23.5	−15.6	832	>100

[a] From dynamic mechanical spectra
[b] From differential scanning calorimetry
[c] Predicted from Fox equation (see text)

poorly defined elastomeric behaviour. The absence of crystallinity reduces the driving force available for phase separation. This is necessary to overcome specific hard–soft segment interactions such as hydrogen bonding that tends to reduce the interaction parameter between the blocks. Crystallinity is not the only mechanism available to increase χ_{AB}. Other specific interdomain interactions such as π-electron attractive forces can also help phase development without crystallinity as shown by Camberlin *et al.*[29] In polyurethane–urea systems, a strong hydrogen bonding (most likely a 3-D arrangement) can explain the phase separation and excellent properties of these polymers without crystallinity.

The absence of intersegmental interactions can make an otherwise compatible system become more phase separated. These have been well illustrated by the work of Cooper *et al.*[30] who have prepared MDI/MDEA based systems using poly(tetramethylene oxide) and polybutadiene based soft segments. Since with PBD soft segments there is no possibility of hard–soft segment hydrogen bonding, these materials show a more complete phase separation than in the PTMO materials.

SUMMARY AND CONCLUSIONS

Through this work we have demonstrated the following points concerning phase separation and properties in bulk RIM polymerized polyurethane elastomers:

(1) The final degree of phase separation, and the molecular weight, in semi-crystalline systems are highly dependent on the rate of polymerization, controlled mainly by the catalyst concentration.

(2) Low reaction rates favour the crystallization of oligomeric materials during the polymerization. Although the samples show a high degree of phase separation and hard segment crystallinity, the heterogeneous conditions of the reaction decrease the molecular weight, resulting in a brittle material with poor tensile properties.

(3) At high reaction rates most of the polymerization takes place before phase separation. The final degree of phase separation and hard segment organization depend mostly on the moulding conditions and thermal history of the material. Under normal RIM conditions the system can be regarded as a finely interconnected network of hard segments dispersed throughout a polyether rich hard segment matrix. This high dispersion of poorly organized hard segments yields a high temperature dependence of the storage modulus.

(4) Increasing the polyol molecular weight increases the length of the segments and increases phase incompatibility. At high enough polyether molecular weight, the effect of catalyst concentration on the temperature dependence of the modulus becomes less apparent.

(5) Comparison between ethanediol and butanediol extenders indicates that the former produces hard segment crystals with a higher melting temperature. Because of higher urethane group concentration in the ethanediol based hard segments, these tend to have higher cohesion thus giving higher T_m.

(6) The use of monomers that produce amorphous hard segments produces highly compatible systems with poorly defined rubbery plateau and elastomeric behaviour. Because no heterogeneous conditions develop during the reaction, molecular weight in amorphous polyurethane systems tends to be less affected by reaction rates of polymerization conditions.

(7) Hard segment crystallizability, and/or other specific interactions such as π-electron forces between aromatic groups or 3-D hydrogen bonding as in polyureas provide higher cohesive intersegmental forces.

ACKNOWLEDGEMENTS

This work was supported by Industry University Cooperative funding from the National Science Foundation, Grant NSF-CPE-8118-232, the General Motors Corporation and the Union Carbide Corporation. The authors are also indebted to Drs D. Spence and J. Ferrarini from Rubicon Chemicals, R. Lloyd from Texaco Chemicals, J. O'Connors from Olin Corp. and R. Gerkin and L. Lawler from Union Carbide for providing us with the raw chemicals used in this work. Invaluable assistance by K. Dulin, J. Horns and J. Andrews in sample preparation and characterization is acknowledged. One of the authors (R.E.C.) would also like to thank the 3M Company for fellowship support through this project.

REFERENCES

1 Gerkin, R. M. and Critchfield, F. E. Paper 741022, Soc. Automotive Engineers Mtg. Toronto, Canada, Oct., 1974
2 Fridman, I. D., Thomas, E. L., Lee, L. J. and Macosko, C. W. *Polymer* 1980, **21**, 393
3 Rice, D. M. and Dominguez, R. J. G. *Polym. Eng. Sci.* 1980, **20**, 1192
4 Dominguez, R. J. G. *Polym. Eng. Sci.* 1981, **21**, 1210
5 Turner, R. B., Spell, H. L. and Vanderhider, J. A. in 'Reaction Injection Molding and Fast Polymerization Reactions', (Ed. J. E. Kresta), Plenum Press, New York, 1982, p. 63
6 Camargo, R. E., Macosko, C. W., Tirrell, M. and Wellinghoff, S. T. *ibid.*, p. 95; *Polym. Eng. Sci.* 1982, **22**, 719
7 Blackwell, J., Quay, J. and Turner, R. B. *Polym. Eng. Sci.* 1983, **23**, 816
8 Kolodziej, P., Macosko, C. W. and Ranz, W. E. *Polym. Eng. Sci.* 1982, **22**, 388

9 Lee, L. J. and Macosko, C. W. *S.P.E. ANTEC Tech. Papers* 1978, **24**, 151; US Patent 4 189 070 (1979)
10 Camargo, R. E. *Ph.D. Thesis*, Dept. of Chemical Engineering and Mat. Sci., U. of Minnesota, 1983
11 Zdrahala, R. J., Gerkin, R. M., Hager, S. L. and Critchfield, F. E. *J. Appl. Polym. Sci.* 1979, **24**, 2041
12 Zhrahala, R. J., Hager, S. L., Gerkin, R. M. and Critchfield, F. E. *J. Elastom. Plast.* 1980, **12**, 225
13 Russo, R. and Thomas, E. L. *J. Macromol. Sci., Phys.* 1983, **B22**, 553
14 Chang, A. L., Briber, R. M., Thomas, E. L., Zdrahala, R. J. and Critchfield, F. E. *Polymer* 1982, **23**, 1060
15 Schneider, N. S., Desper, C. R., Illinger, J. R. and King, A. O. *J. Macromol. Sci., Phys.* 1975, **B11**, 527
16 Seymour, R. W. and Cooper, S. L. *Macromolecules* 1973, **6**, 48
17 Hesketh, T. R., Van Bogart, J. W. C. and Cooper, S. L. *Polym. Eng. Sci.* 1980, **20**, 190
18 Lopez-Serrano, F., Castro, J. M., Macosko, C. W. and Tirrell, M. *Polymer* 1980, **21**, 263
19 Tirrell, M., Lee, L. J. and Macosko, C. W. *A.C.S. Symp. Series* 1979, **104**, 149
20 Xu, M., MacKnight, W. J., Chen, C. H. Y. and Thomas, E. L. *Polymer* 1983, **24**, 1327
21 Saunders, J. H. *Rubber Chem. Technol.* 1960, **33**, 1259
22 Mirabella, F. M., Northern Petrochemical Co., personal comm., 1983
23 Hashimoto, T., Tsukahara, Y., Tachi, K. and Kawai, H. *Macromolecules* 1983, **16**, 648
24 Kojima, H., Nishimura, H. and Funaki, M. *Reports Res. Lab. Asahi Glass Co.* 1981, **31**, 109
25 Briber, R. M. and Thomas, E. L. *J. Macromol. Sci., Phys.* 1983, **B22**, 509
26 Blackwell, J. and Lee, C. D. *J. Polym. Sci. Polym. Phys. Edn* 1984, **22**, 759
27 Billmeyer, F. W. 'Principles of Polymer Science', 2nd Edn., Wiley, 1984
28 Hwang, K. K. S., Yang, C. Z. and Cooper, S. L. *Polym. Eng. Sci.* 1981, **21**, 1027
29 Camberlin, Y., Pascault, P., Letoffe, M. and Claudy, P. *J. Polym. Sci., Polym. Chem. Edn.* 1982, **20**, 1445
30 Yang, C. Z., Hwang, K. K. S. and Cooper, S. L. *Markomol. Chem.* 1983, **184**, 651